Engineering Research Express

PAPER

Modelling and numerical analysis of ZnO/CuO/Cu_2O heterojunction solar cell using SCAPS

To cite this article: Nguyen Dinh Lam 2020 *Eng. Res. Express* **2** 025033

Engineering Research Express

PAPER

Modelling and numerical analysis of ZnO/CuO/Cu_2O heterojunction solar cell using SCAPS

RECEIVED
20 March 2020

REVISED
10 May 2020

ACCEPTED FOR PUBLICATION
27 May 2020

PUBLISHED
4 June 2020

Nguyen Dinh Lam

Faculty of Engineering Physics and Nanotechnology, VNU-University of Engineering and Technology, Vietnam National University, 144, Xuanthuy, Caugiay, Hanoi, Vietnam

E-mail: lamnd2005@gmail.com

Keywords: buffer layer, ZnO/CuO/Cu_2O, heterojunction, solar cells

Abstract

In this work, the SCAPS-1D program was utilized to perform simulations of ZnO/CuO/Cu_2O thin-film solar cells. Based on the cell structure and device fabrication process, solar cell structure parameters such as the thickness of the CuO layer, ZnO layer, donor density in the ZnO layer were evaluated in detail. The results indicated that an optimal structure of ZnO/CuO/Cu_2O thin-film solar cell could be obtained when the thickness of the ZnO layer, CuO layer, and donor density in the ZnO layer is 100 nm, 500 nm, 1×10^{17} cm^{-3}, respectively. The optimized solar cell structure of ZnO/CuO/Cu_2O shows a potential efficiency of about 12% under the 1 sun air mass 1.5 G spectrum illumination. Besides that, the performance of the cell under individual solar concentrations and operating temperatures was also investigated.

1. Introduction

Semiconductor materials, that are created from metal oxides, are abundant, chemically stable, and, non-toxic. These kinds of materials are promising materials for optoelectronic devices fabrication [1–5]. Active or passive components in a broad range of commercial applications, such as active channel layers in solar cells as transparent conducting front electrodes and as electron or hole transport layers [6] or in the transistors that constitute active-matrix displays [7], were usually made by metal oxide materials. Besides some structures of photovoltaic cells [8–10], heterojunctions entirely based on metal oxides, so called all-oxide photovoltaic cells, have recently attracted considerable attention because of their promising potential to reduce photovoltaic prices due to their low cost, abundant, and inexpensive production methods [11–13].

Cupric oxide (CuO), a black solid stable oxide of copper, has a bandgap of 1.2 eV, a p-type transitional metal oxide semiconductor property, monoclinic crystal structure with adsorption coefficient 105 cm^{-1}, the electrical resistivity of about 10 to 105 Ω.cm and high thermal conductivity [14–17]. CuO material has numerous benefits, including high prevalence, low-cost, nontoxicity, comparatively simple preparation process, and individual square planar coordination of copper and oxygen [18]. CuO is widely utilized as an active layer in some kinds of photovoltaic structures [19–21]. The highest power conversion efficiency of solar cells based on the CuO material can be obtained up to 3.82% [20].

Zinc oxide material (ZnO) is a direct-wide bandgap semiconductor of 3.34 eV and has a high potential for use in electronics and opto-electronics due to its transparency in the visible spectral region [1, 2]. Furthermore, ZnO can be easily formed under one-dimension nanostructures [22–25] and greatly abundant in nature with low costs.

The CuO/ZnO heterojunction is frequently used in solar cells, sensors, and photocatalytic applications. To date, however, heterojunction solar cells based on ZnO/CuO heterojunction have achieved an efficiency of only 3.83% [26].

Numerical simulations of solar cells using Solar Cell Capacitance Program (SCAPS-1D) have been reported on some kinds of solar cell structures such as CdS/CdTe solar cells [27], CdTe and Cu(In, Ga)Se2 solar cells [28],

Table 1 Parameters of ZnO, CuO, and Cu_2O [30–36].

Parameter	ZnO	CuO	Cu_2O
Thickness, d(nm)	**Varied**	**Varied**	30
Bandgap, Eg (eV)	3.2	1.3	2.1
Electron affinity E_A(eV)	4.3	4.07	3.2
Relative dielectric permittivity $\varepsilon_{n,p}$	9	18.1	7.1
Conduction band effective density of states N_C (cm^{-3})	2.2×10^{18}	1×10^{19}	1×10^{19}
Valance band effective density of states N_V (cm^{-3})	1.8×10^{18}	1×10^{19}	1×10^{19}
Electron mobility ($cm^2\ V^{-1}\ s^{-1}$)	100	100	200
Hole mobility ($cm^2\ V^{-1}\ s^{-1}$)	25	0.1	80
Shallow uniform donor density N_D (cm^{-3})	**Varied**	0	0
Shallow uniform acceptor density N_A (cm^{-3})	0	1×10^{16}	1×10^{15}

n-TiO_2/p-CuO and n-TiO_2/p-Cu_2O heterojunction solar cells [29], etc. The results were in agreement with experimental reported works.

Here, the simulated thin-film planar ZnO/CuO/Cu_2O solar cell was modeled. The thickness of the CuO layer, ZnO layer, donor density in the ZnO layer was evaluated in detail. All proposed layer thickness is provided by the technological conditions of thin-film manufacturing. The results indicated that a numerical simulation is a valuable tool for the theoretical analysis of thin-film solar cells that can provide insight into the internal physics and operations of solar cells.

2. Methods

The SCAPS performs a complete simultaneous numerical solution of the two continuity equations and Poisson's equation conditional on the boundary conditions appropriate to one and two-dimensional cells. The equations are expressed as shown in equations (1)–(3).

$$\nabla^2 v = -q/\in (p - n + N_D - N_A) \tag{1}$$

$$\nabla . J_p = q(G - R) \tag{2}$$

$$\nabla . J_n = q(R - G) \tag{3}$$

The general terms of equations (2) and (3) can be represented as:

$$G(x) = \int_0^\infty \phi\alpha e^{-\alpha x} d\lambda \tag{4}$$

The hole and electron current densities which appear in equations (2) and (3) are given by

$$J_p = -q\mu_p p\nabla V_p - kT\mu_p \nabla_p \tag{5}$$

$$J_n = -q\mu_n n\nabla V_n + kT\mu_n \nabla_n \tag{6}$$

$$V_p = V - (1 - \gamma)\Delta G/g \tag{7}$$

$$V_n = V + \gamma\Delta G/g \tag{8}$$

where v_p and v_n represent the effective potentials expressed in equations (7) and (8). ΔG and γ account for variations in the band structure, such as the density of band gap and states, and account for Fermi–Dirac statistics. Expression J_n and J_p represent the current density of the electron and holes, respectively. Similarly, μ_n and μ_p represent the mobility of electron and hole, respectively.

SCAPS (version 3.3.07) was used to simulate the J–V, C-V, QE photovoltaic characteristics of the thin-film planar ZnO/CuO/Cu_2O solar cell. Based on these characteristics, the most important parameters such as short-circuit current density (J_{sc}), open circuit voltage (V_{oc}), fill factor (FF), and power conversion efficiency (η) under standard illumination (AM 1.5 G, 100 mW cm^{-2}, 300 K) were calculated and analyzed. The properties of the materials used in the simulations were acquired from the literature [30–36]. The parameters for Cu_2O, CuO, and ZnO used in the simulations are provided in table 1. The parameters for the back and front contacts of the solar cell are provided in table 2. Figure 1 shows the constructed thin-film planar ZnO/CuO/Cu_2O heterojunction solar cell structure used for the SCAPS simulations. The influences of the layer thickness of CuO and ZnO were analyzed. Additionally, the influence of the shallow uniform donor density that was varied from 10^{15} cm^{-3} to 10^{21} cm^{-3} in the ZnO layer with a constant shallow uniform acceptor density (10^{17} cm^{-3}) for CuO was also evaluated. Finally, based on the optimized structure of the thin-film planar ZnO/CuO/Cu_2O heterojunction solar cell, the performance of the cell under individual solar concentrations and operating temperatures was also investigated.

Table 2. Parameters of back and front contacts.

Parameters	Back contact (Cu)	Front contact (Ag)
Surface recombination velocity of electrons ($cm.s^{-1}$)	1.0	1×10^7
Surface recombination velocity of holes ($cm.s^{-1}$)	1×10^7	1.0
Metal work function (eV)	4.6	4.7

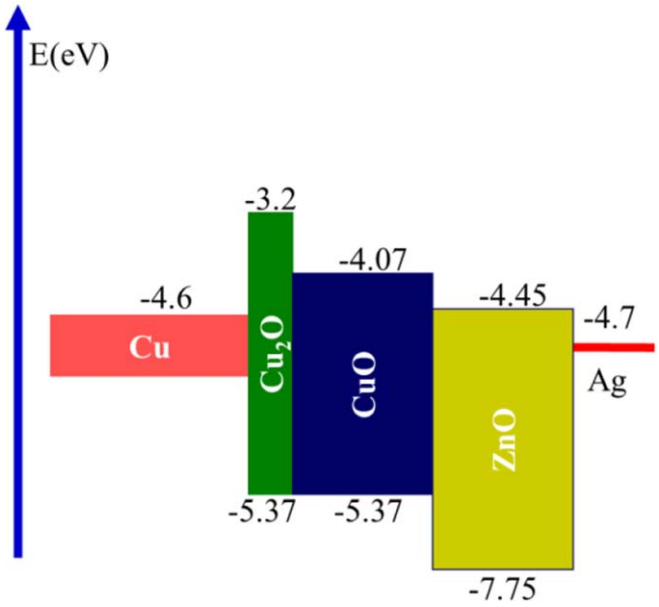

Figure 1. Schematic of the thin-film planar ZnO/CuO/Cu_2O heterojunction solar cell.

3. Simulation of thin-film planar ZnO/CuO/Cu_2O heterojunction solar cell

Simulation of the thin-film planar ZnO/CuO/Cu_2O heterojunction solar cells was performed without introducing additional defects. The thickness of each layer was controlled as 100 nm, 500 nm, and 30 nm for the ZnO, CuO, and Cu_2O layers, respectively. The shallow donor density in the ZnO layer was set as 10^{16} cm^{-3}. The shallow acceptor densities in the CuO and Cu_2O were set as 10^{16} cm^{-3} and 10^{15} cm^{-3}, respectively. The J–V and P-V characteristics for the ZnO/CuO/Cu_2O heterojunction solar cells were shown in figure 2. Based on this structure, the short circuit current density can be obtained up to 27.4 $mA.cm^{-2}$ resulting in obtained 10.6% in power conversion efficiency. It could be concluded that this thin-film planar ZnO/CuO/Cu_2O heterojunction structure works well in the photo-conversion process for solar cells. In the following section, based on the ZnO/CuO/Cu_2O heterojunction structure, the influences of the thickness of ZnO and CuO layers, shallow donor density in ZnO layer, that can be controlled by the real device fabrication processes, will be evaluated various approaches to find out an optimum structure.

4. Influence of thickness of the ZnO layer

The ZnO is an n-type buffer layer in the thin-film planar ZnO/CuO/Cu_2O heterojunction structure. For minimizing the series resistance of the PV device, the thickness of the buffer layer should be as thin as possible [37]. In this work, for investigation the influences of the thickness of ZnO layer, the thickness of the CuO, Cu_2O layers and shallow donor density in ZnO, CuO, Cu_2O layers were kept as constants of 300 nm, 30 nm, 1×10^{16} cm^{-3}, 1×10^{16} cm^{-3}, and 1×10^{15} cm^{-3}, respectively. The solar cell parameters (V_{oc}, J_{sc}, FF, and η) and quantum efficiency characteristics were generated based on the variation of the thickness of ZnO layer and depicted in figures 3 and 4. The V_{oc}, J_{sc} were reduced as increasing in the thickness of ZnO n-type buffer layer resulting in the reduction of power conversion efficiency. This can be attributed to the shallow penetration of UV light which is absorbed by the ZnO layer. Based on the QE result, the optimal thickness of ZnO n-type buffer layer could be chosen to be 100 nm corresponding to a cell efficiency of 10.63%.

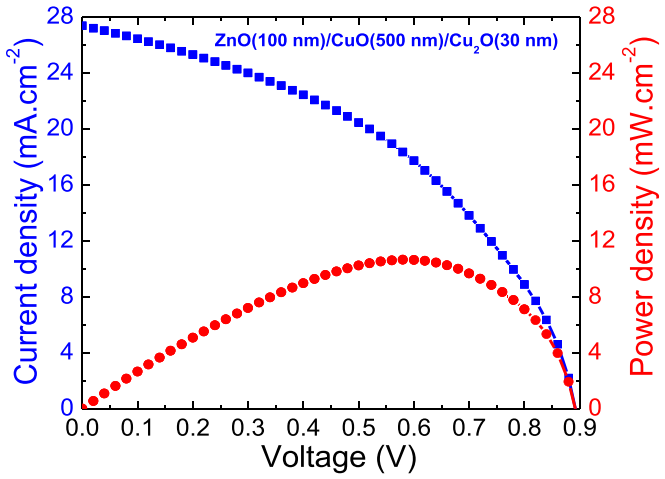

Figure 2. The J–V and P-V characteristics for the ZnO/CuO/Cu_2O heterojunction solar cells.

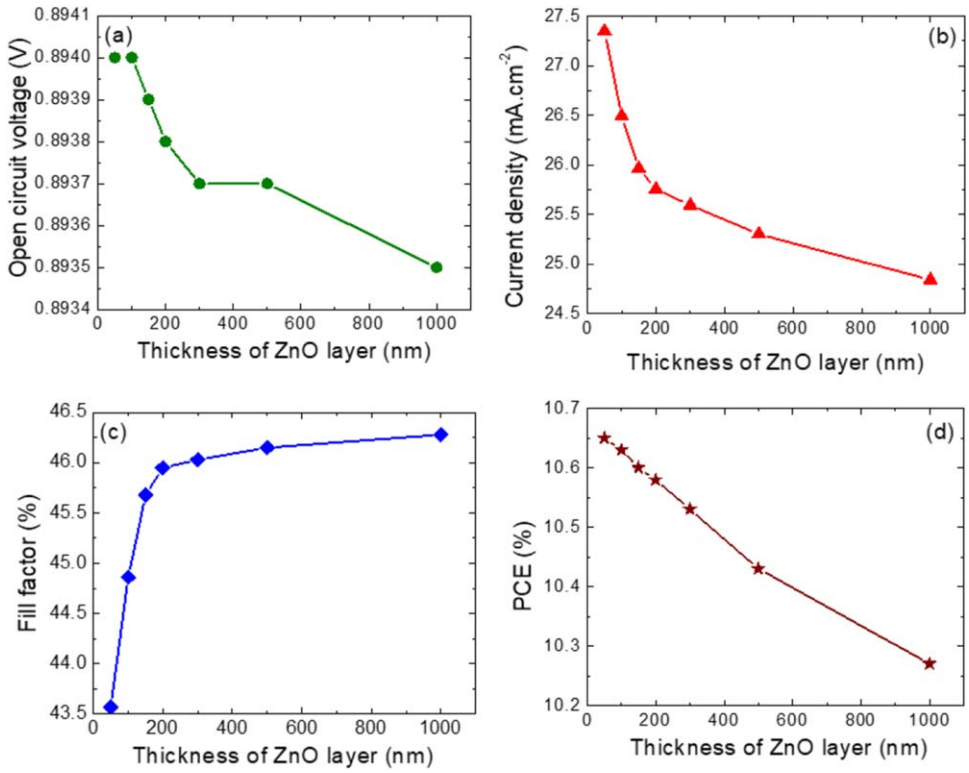

Figure 3. The influences of ZnO n-type buffer layer thickness on the cell parameters.

5. Influence of thickness of the CuO layer

The CuO is a p-type absorber layer in the thin-film planar ZnO/CuO/Cu_2O heterojunction structure. The absorber layer is the most important component of the solar cell where the incident photons are absorbed and excess carriers are generated. In this work, the influence of the CuO p-type absorber layer thickness on the thin-film planar ZnO/CuO/Cu_2O heterojunction solar cell parameters are simulated by changing the thickness from 100 to 1000 nm without introducing additional defects. The thickness of the ZnO, Cu_2O layers, and shallow donor density in ZnO, CuO, Cu_2O layers were kept as constants of 100 nm, 30 nm, 1×10^{16} cm^{-3}, 1×10^{16} cm^{-3}, and 1×10^{15} cm^{-3}, respectively.

The solar cell parameters (V_{oc}, J_{sc}, FF, and η) and quantum efficiency characteristics were generated based on the variation in the thickness of CuO layer and depicted in figures 5 and 6. The results indicated that the J_{sc} and η parameters of the thin-film planar ZnO/CuO/Cu_2O heterojunction solar cell increase initially with an increase

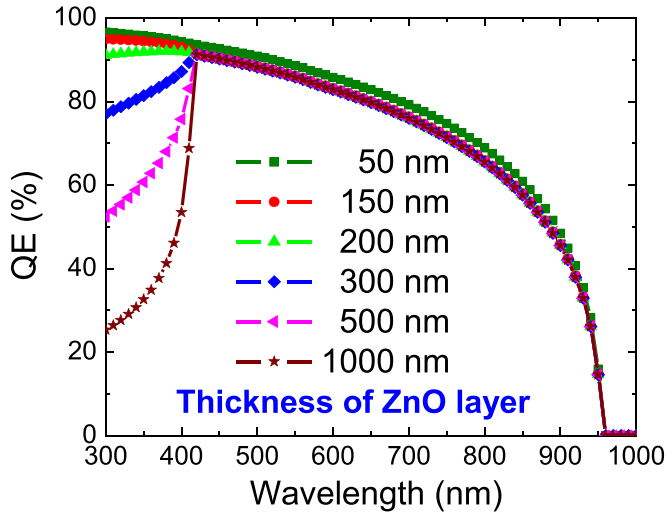

Figure 4. The influences of ZnO n-type buffer layer thickness on the quantum efficiency.

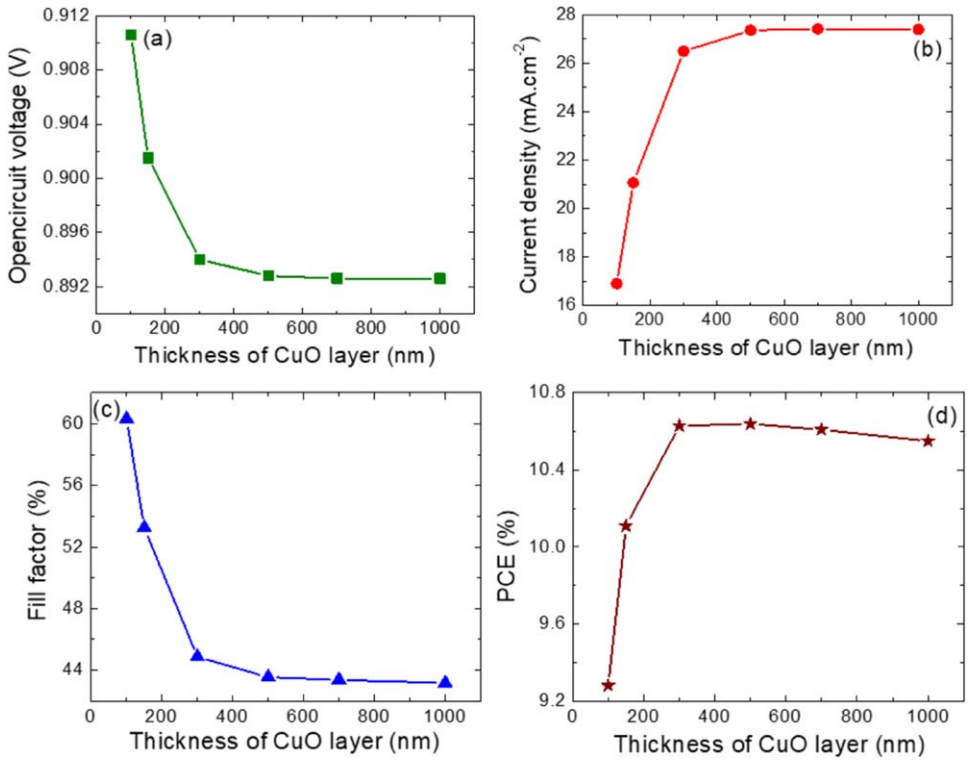

Figure 5. The influences of CuO p-type absorber layer thickness on the cell parameters.

in the thickness of the CuO p-type absorber layer up to 500 nm and nearly saturates at higher values. Which are mainly attributed to the enhanced absorption of incident light due to the thickness of the absorber layer [37]. As the thickness of the CuO layer increasing, the layer can absorb more photons, resulting in an increased photo-generated current. The saturation in solar cell parameters could be attributed to the increased probability of SRH (Shockley-Read-Hall) recombination (due to finite carrier diffusion length) with an increase in absorber thickness. Moreover, a thicker absorber layer will take disadvantage in higher material cost and fabrication cost [37]. Therefore, in this work, the optimized thickness for CuO p-type absorber layer is 500 nm.

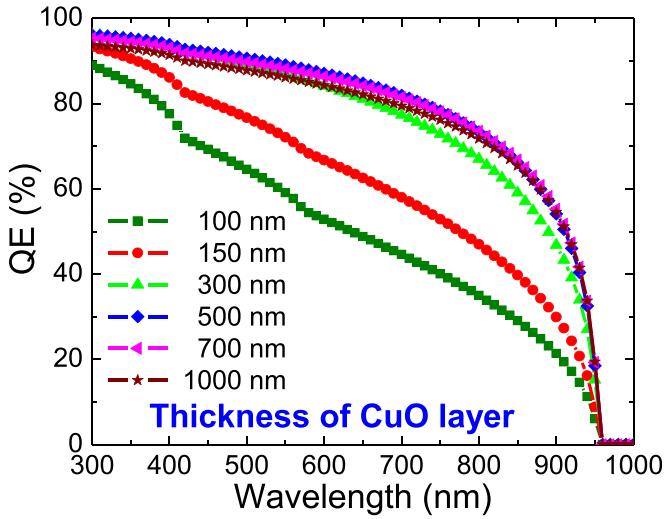

Figure 6. The influences of CuO p-type absorber layer thickness on the quantum efficiency.

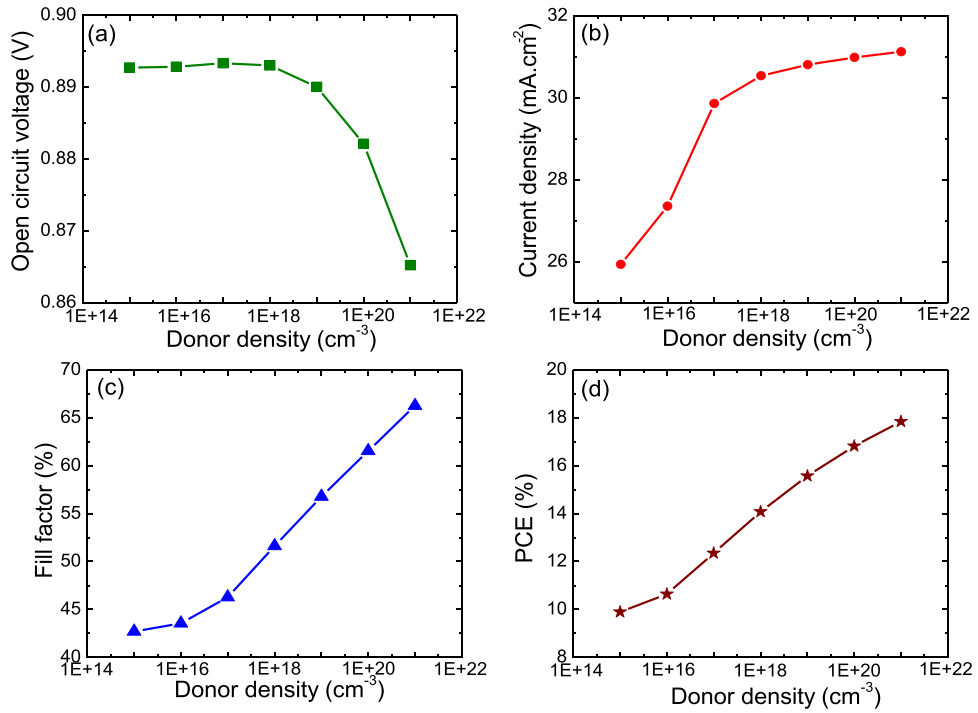

Figure 7. The influences of shallow donor density on the cell parameters.

6. Influence of the shallow donor density in ZnO layer

The shallow donor density values varied in the range from 10^{15} cm^{-3} to 10^{21} cm^{-3} for the ZnO layer with a constant uniform acceptor doping density of N_A 10^{16} cm^{-3} for the CuO layer (Figure.7). The J_{sc} parameter of the thin-film planar ZnO/CuO/Cu_2O heterojunction solar cell increases initially with an increase in the shallow donor density up to 10^{17} cm^{-3} and nearly saturates at higher values. However, the V_{oc} value was nearly no change as the shallow donor density increases up to 10^{18} cm^{-3} and dropped as the higher shallow donor density. Therefore, in this work, the optimized shallow donor density is 10^{17} cm^{-3}.

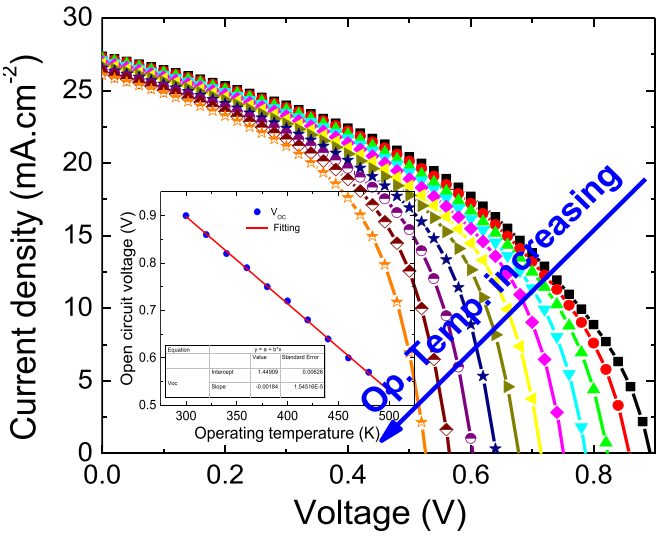

Figure 8. J-V curves of the thin-film planar ZnO/CuO/Cu_2O heterojunction solar cell versus operating temperature.

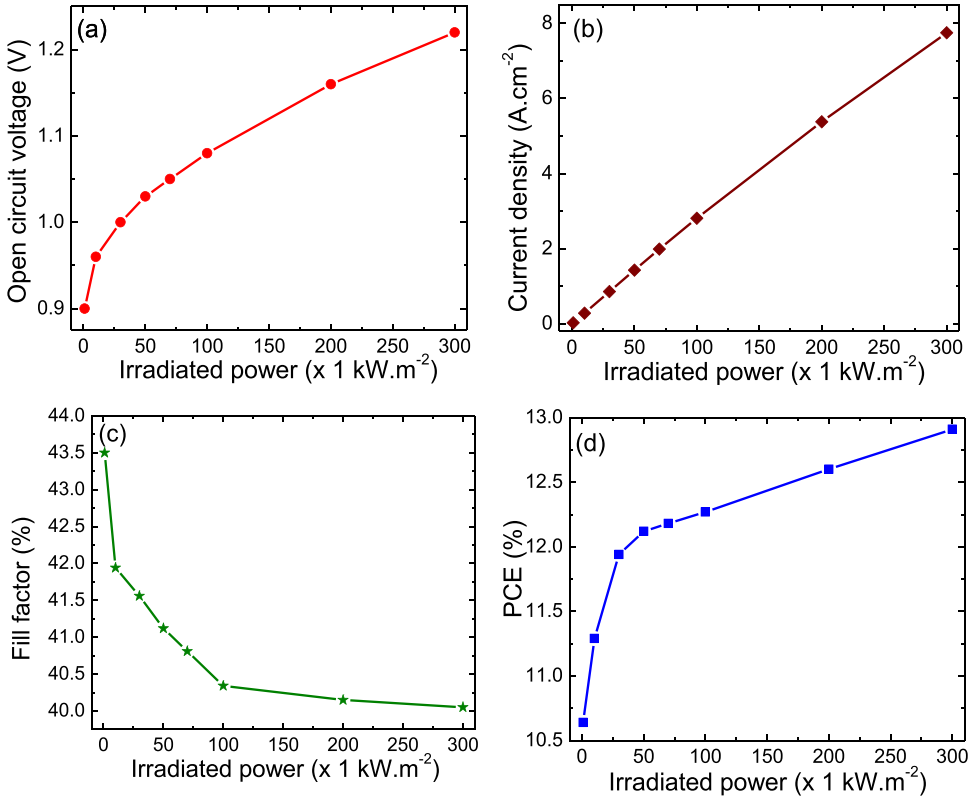

Figure 9. The influences of solar concentration on the cell parameters.

7. Influence of operating temperature

Figure 8 shows the results of J-V curves for the thin-film planar ZnO/CuO/Cu_2O heterojunction solar cell operated under different temperatures. The V_{oc} of the cell strongly depends on the operating temperature. The V_{oc} is as lower as higher operating temperature.

8. Influence of solar concentration

Figure 9 shows the influence of solar concentration on solar cell parameters. The solar concentration varied from 1 sun to 300 suns that related to the irradiated power from 1 kW.cm^{-2} to 300 kW.cm^{-2}. The η parameter of the solar cell rapidly increases with an increase in the irradiated power up to 70 kW.m^{-2} and slowly increases at higher values. This indicated that the thin-film planar ZnO/CuO/Cu_2O heterojunction solar cell could be operated under high irradiated power and work well under 70 suns condition.

9. Conclusions

In this work, the thin-film planar ZnO/CuO/Cu_2O heterojunction solar cell was investigated using the solar cell simulator, SCAPS. The structure of solar cell was optimized for different parameters such as the thickness of n-type buffer layer—ZnO, p-type absorber layer—CuO, the shallow donor density, and working under various operating temperatures and solar concentration based on the analysis of J-V characteristics and Quantum efficiency.

On the simulation basis, it was demonstrated that the thickness of the buffer and absorber layers, shallow donor density affect strongly on the cell performance. The optimized structure could be obtained with 100 nm thick and 10^{17} cm^{-3} shallow donor density of the ZnO n-type buffer layer, 500 nm thick of CuO p-type absorber layer. Furthermore, the best operating conditions of the thin-film planar ZnO/CuO/Cu_2O heterojunction solar cell is at the working point at 300 K and 70 Sun corresponding to the power conversion efficiency of 12.18%.

The optimized structure obtained from this simulation model will offer an instruction in the fabrication and optimization of the thin-film planar ZnO/CuO/Cu_2O heterojunction solar cell.

Acknowledgments

The authors are thankful to Prof. Marc Burgelman, University of Gent, Belgium for providing the SCAPS software for our study. This research is funded by Vietnam National University, Hanoi (VNU) under project number QG.19.20.

ORCID iDs

Nguyen Dinh Lam https://orcid.org/0000-0002-4349-6830

References

[1] Mizuno J, Jeem M, Takahashi Y, Kawamoto M, Asakura K and Watanabe S 2020 Light and shadow effects in the submerged photolytic synthesis of micropatterned CuO nanoflowers and ZnO nanorods as optoelectronic surfaces *ACS Appl. Nano Mater.* **3** 1783–91
[2] Mahajan P, Singh A and Arya S 2019 Improved performance of solution processed organic solar cells with an additive layer of sol-gel synthesized ZnO/CuO core/shell nanoparticles *J. Alloys Compd.* **814** 152292
[3] Yin W, Yang J, Zhao K, Cui A, Zhou J, Tian W and Chu J 2020 High responsivity and external quantum efficiency photodetectors based on solution-processed Ni-doped CuO films *ACS Appl. Mater. Interfaces* 2020 **12** 11797–805
[4] Nguyen T T, Patel M, Kim J-W, Lee W and Kim J 2019 Functional TiO_2 interlayer for all-transparent metal-oxide photovoltaics *J. Alloys Compd.* **816** 152602
[5] Koc M M 2020 Photoelectrical properties of solar sensitive CuO doped carbon photodiodes *J. Mol. Struct.* **1208** 127872
[6] Fortunato E, Ginley D, Hosono H and Paine D C 2007 Transparent conducting oxides for photovoltaics *MRS Bull.* **32** 242–7
[7] Fortunato E, Barquinha P and Martins R 2012 Oxide semiconductor thin-film transistors: a review of recent advances *Adv. Mater.* **24** 2945–86
[8] Tsunomura Y, Yoshimine Y, Taguchi M, Baba T, Kinoshita T, Kanno H, Sakata H, Maruyama E and Tanaka M 2009 Twenty-two percent efficiency HIT solar cell *Solar Energy Materials & Solar Cells* **93** 670–3
[9] Ajmal Khan M, Sato R, Sawano K, Sichanugrist P, Lukianov A and Ishikawa Y 2018 Growth and characterization of low composition Ge, x in epi-Si1-xGex (x ⩽ 10%) active layer for fabrication of hydrogenated bottom solar cell *J. Phys. D: Appl. Phys.* **51** 185107
[10] Ajmal Khan M and Suemasu T 2017 Donor and acceptor levels in impurity-doped semiconducting BaSi2 thin films for solar-cell application *Phys. Status Solidi* A **214** 1700019
[11] Morasch J, Li S, Brötz J, Jaegermann W and Klein A 2014 Reactively magnetron sputtered Bi2O3 thin films: analysis of structure, optoelectronic, interface, and photovoltaic properties *Phys. Status Solidi* (A) **211** 93–100
[12] Wisz G, Nykyruy L, Yakubiv V, Hryhoruk I and Yavorskyi R 2018 Impact of advanced research on development of renewable energy policy: case of Ukraine *International Journal of Renewable Energy Research (IJRER).* **8** 2567–2584
[13] Ruhle S, Anderson A Y, Barad H N, Kupfer B, Bouhadana Y, Rosh-Hodesh E and Zaban A 2012 All-oxide photovoltaics *The Journal of Physical Chemistry Letters.* **3** 3755–64
[14] Shabu R *et al* 2015 Assessment of CuO thin films for its suitability as window absorbing layer in solar cell fabrications *Mater. Res. Bull.* **68** 1–8
[15] Ooi P K *et al* 2013 Effects of oxygen percentage on the growth of copper oxide thin films by reactive radio frequency sputtering *Mater. Chem. Phys.* **140** 243–8

[16] Valladares L D L S *et al* 2012 Crystallization and electrical resistivity of Cu2O and CuO obtained by thermal oxidation of Cu thin films on SiO2/Si substrates *Thin Solid Films* **520** 6368–74
[17] Liu M, Lin M C and Wang C 2011 Enhancements of thermal conductivities with Cu, CuO, and carbon nanotube nanofluids and application of MWNT/water nanofluid on a water chiller system *Nanoscale Res. Lett.* **6** 297
[18] Figueiredo V, Elangovan E, Goncalves G, Barquinha P, Pereira L, Franco N, Alves E, Martins R and Fortunato E 2008 Effect of postannealing on the properties of copper oxide thin films obtained from the oxidation of evaporated metallic copper *Appl. Surf. Sci.* **254** 3949–54.
[19] Kidowaki H, Oku T and Akiyama T 2012 Fabrication and characterization of CuO/ZnO solar cells *J. Phys. Conf. Ser.* **352** 012022
[20] Siddiqui H, Parra M R, Pandey P, Qureshi M S and Haque F Z 2020 Utility of copper oxide nanoparticles (CuO-NPs) as efficient electrondonor material in bulk-heterojunction solar cells with enhancedpower conversion efficiency *Journal of Science: Advanced Materials and Devices* **5** 104–10
[21] Kaphle A, Echeverria E, Mcllroy D N and Hari P 2020 Enhancement in the performance of nanostructured CuO–ZnO solar cells by band alignment *RSC Adv.* **10** 7839–54
[22] Braiek Z, Roques-Carmes T, IBen A, Gannouni M, Arnoux P, Corbel S and Chtourou R 2018 Enhanced solar and visible light Photocatalytic activity of In2S3-Decorated ZnO Nanowires for water purification *Journal of Photochemistry and amp; Photobiology, A: Chemistry* **368** 307–16
[23] Jiang Y, Liao J-F, Xu Y-F, Chen H-Y, Wang X-D and Kuang D-B 2019 Hierarchical $CsPbBr_3$ nanocrystal decorated ZnO nanowires/ macroporous graphene hybrids for enhancing charge separation and photocatalytic CO_2 reduction *J. Mater. Chem.* A **7** 13762–9
[24] Smazna D, Shree S, Polonskyi O, Lamaka S, Baum M, Zheludkevich M, Faupel F, Adelung R and Mishra Y K 2019 Mutual interplay of ZnO Micro- and nanowires and methylene blue during cyclic photocatalysis process *Journal of Environmental Chemical Engineering* **7** 103016
[25] Singh R and Dutta S 2019 The role of pH and nitrate concentration in the wet chemical growth of nano-rods shaped ZnO photocatalyst *Nano-Structures & Nano-Objects* **18** 100250
[26] Minami T, Nishi Y, Miyata T and Nomoto J-L 2011 High-efficiency oxide solar cells with ZnO/Cu_2O heterojunction fabricated on thermally oxidized Cu_2O sheets *Appl. Phys. Exp.* **4** 062301
[27] Anwar F, SarwarSatter S, Mahbub R, Mahmud Ullah S and Afrin S 2017 Simulation and performance study of nanowire CdS/CdTe solar cell *International Journal of Renewable Energy Research.* **7** 885–893
[28] Burgelman M, Nollet P and Degrave S 2000 Modelling polycrystalline semiconductor solar cells *Thin Solid Films* **361** 527–32
[29] Sawicka-Chudy P, Sibiński M, Wisz G, Rybak-Wilusz E and Cholewa M 2018 Numerical analysis and optimization of Cu_2O/TiO_2, CuO/TiO_2, heterojunction solar cells using SCAPS *Journal of Physics.* **1033** 012002
[30] Gou L and Murphy C 2002 Solution-phase synthesis of Cu_2O nanocubes *J. Nano Lett.* **3** 231–4
[31] Wang W Z, Wang G H, Wang X S, Zhan Y J, Liu Y K and Zheng C L 2002 Synthesis and characterization of Cu_2O nanowires by a novel reduction route *Adv. Mater.* **14** 67–9
[32] Liao L *et al* 2009 P-type electrical, photoconductive, and anomalous ferromagnetic properties of Cu_2O nanowires *Appl. Phys. Lett.* **94** 113106–113106
[33] Gelczuk Ł, Dąbrowska-Szata M and Jóźwiak G 2005 Distinguishing and identifying point and extended defects in DLTS measurements *Materials Science-Poland* **23** 625–641
[34] Srikant V and Clarke D R 1998 On the optical band gap of zinc oxide *J. Appl. Phys.* **83** 5447
[35] Sohn J *et al* 2013 Engineering of efficiency limiting free carriers and an interfacial energy barrier for an enhancing piezoelectric generation *Energy Environ. Sci.* **6** 97–104
[36] Anwar F, Mahbub R, Satter S S and Ullah S M 2017 Effect of different HTM layers and electrical parameters on ZnO nanorod-based lead-free perovskite solar cell for high-efficiency performance *Int. J. Photoenergy* **2017** 9846310
[37] Sawicka-Chudy P, Starowicz Z, Wisz G, Yavorskyi R, Zapukhlyak Z, Bester M, Głowa M, Sibiński and Cholewa M 2019 Simulation of TiO_2/CuO solar cells with SCAPS-1D software *Mater. Res. Express* **6** 085918